# Supporting Information

# Machine learning-assisted Cu-MOF/OPD/RB triple-emission ratio fluorescence sensing platform for the detection and discrimination of glutathione

Shiwen Wu[ab], Shuqi Wang[ab], Hui Xie[c], Yaxin Li[ab], Hongzhi Lu[a], Shuzhen Zheng[a], Shuai Sun[b], Shoufang Xu[b]*

[a] School of Chemistry and Chemical Engineering, Linyi University, Linyi 276005, China

[b] Laboratory of Functional Polymers, School of Materials Science and Engineering, Linyi University, Linyi 276005, China

[c] China Unicom Communications Co., LTD. Jinan Software Research Institute, Huanenglu, Jinan, 250100, China

*** Corresponding author, E-mail shfxu1981@163.com (S.F. Xu)**

# 1. Materials and apparatus

## 1.1 Materials

Glutathione (GSH, 98%), 2-amino-1,4-benzenedicarboxylic acid (1,4-BDC-NH2, ≥98%), Rhodamine B (RB, AR) were sourced from Aladdin Biochemical Technology Co., Ltd. located in Shanghai. o-phenylenediamine (OPD, ≥98%), ascorbic acid (AA), cysteine (Cys), citric acid (CA), Vitamin A (VitA), were all acquired from Shanghai Macklin Biochemical Co., Ltd. (Shanghai, China). uric acid(UA), Copper nitrate trihydrate ($Cu(NO_3)2{\cdot}3H_2O$, 99%), sodium chloride (NaCl), magnesium sulfate ($MgSO_4$), calcium carbonate ($CaCO_3$), potassium dihydrogen phosphate ($KH_2PO_4$), Iron(III) chloride hexahydrate ($FeCl_3{\cdot}6H_2O$), Zinc sulfate Heptahydrate ($ZnSO_4{\cdot}7H_2O$), were all acquired from Shanghai Zhanyun Chemical Co., Ltd. All solutions were prepared using distilled water.

## 1.2. Apparatus

The fluorescence spectra were recorded using a Fluoromax-4 spectrophotometer provided by Horiba Scientific. Scanning electron microscopy (SEM) images was obtained with a SEM 5000 field emission electron microscope. X-ray diffraction (XRD) pattern was obtained with a SmartLab3000 dif-fractometer. Fourier transform infrared (FT-IR) spectra were performed with Nicolet IS5 spectrometer and the UV-visible absorption spectra were obtained by a UV-3600 ultraviolet spectrophotometer from Shimadzu, Japan. Fluorescence images were taken by AGL-9406 portable UV lamp.

## 2. The purification steps of Cu-MOF

The precipitate obtained by centrifugation was washed with DMF (3 times, 10 mL), anhydrous ethanol (3 times, 10 mL), and deionized water (3 times, 10 mL). After each washing, the precipitate was centrifuged at 8000 rpm for 10 min to fully remove the unreacted monomer and solvent.

## 3. Characterizations of Cu-MOF

### 3.1 The stability of Cu-MOF

As shown in Figure S1, the fluorescence intensity of Cu-MOF has no obvious change in the aqueous phase system of pH 5.7 ~ 8.0, and it is stable in 0.1 ~ 0.5 mM NaCl solution. The fluorescence intensity of Cu-MOF measured within one week of storage has no significant effect. In addition, three batches of Cu-MOF were prepared, and the fluorescence intensity measured under the same conditions was basically the same, which proved that the repeatability between batches was good.

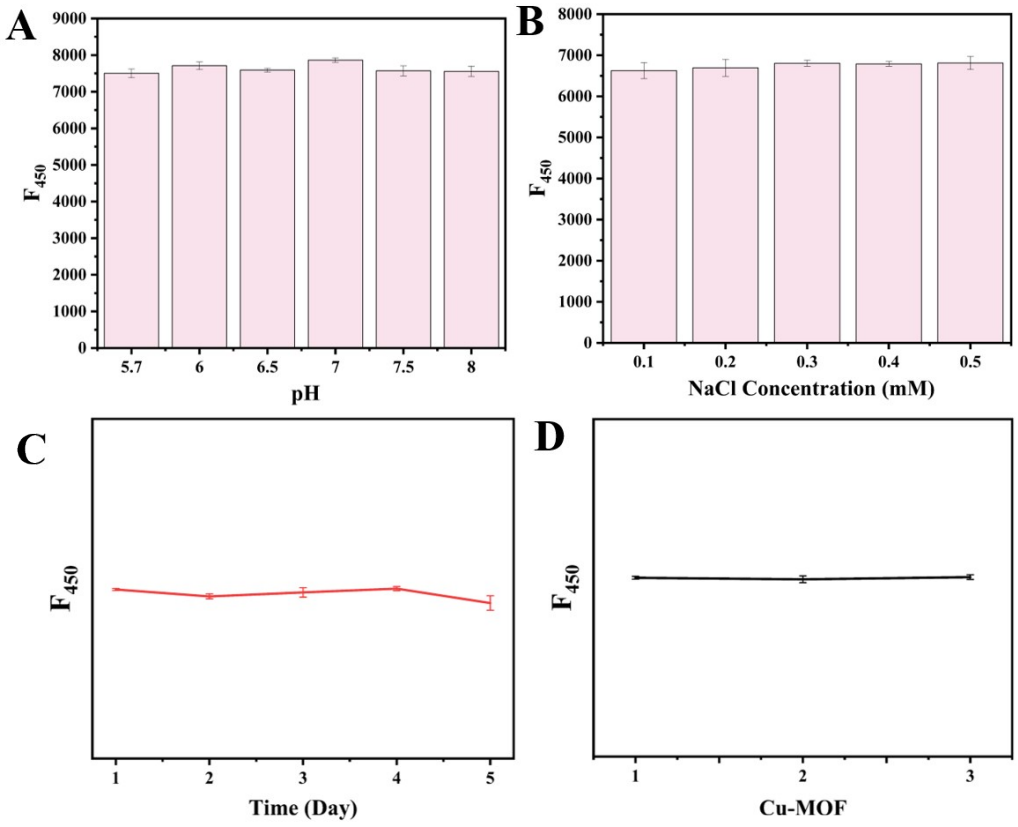


Fig.S1 The stability of Cu-MOF at different pH values (A) and ionic strengths (B),

storage stability (C) and repeatability between batches (D).

### 3.2 XPS spectra of Cu-MOF

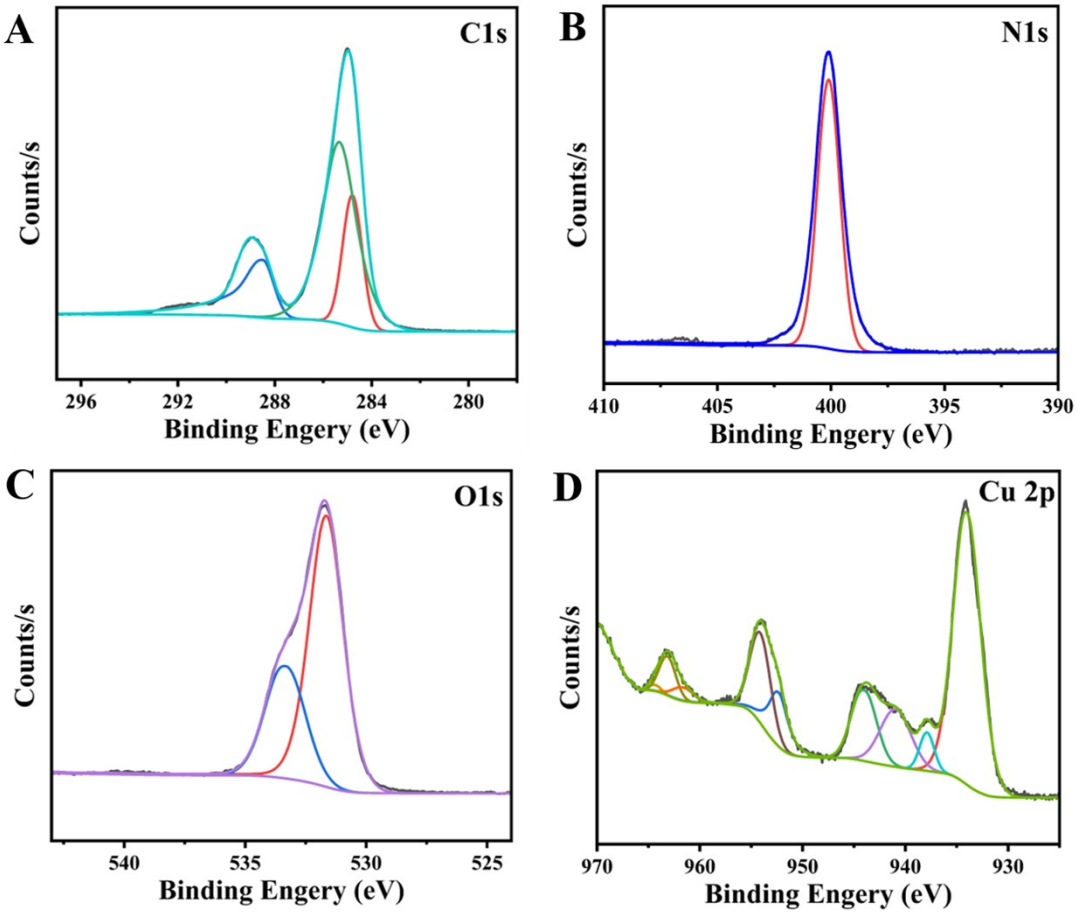


Fig.S2 C1s (A); N1s (B); O1s (C) and Cu2p (D)XPS spectra of Cu-CDs.

## 4. POD-like activity of Cu MOF

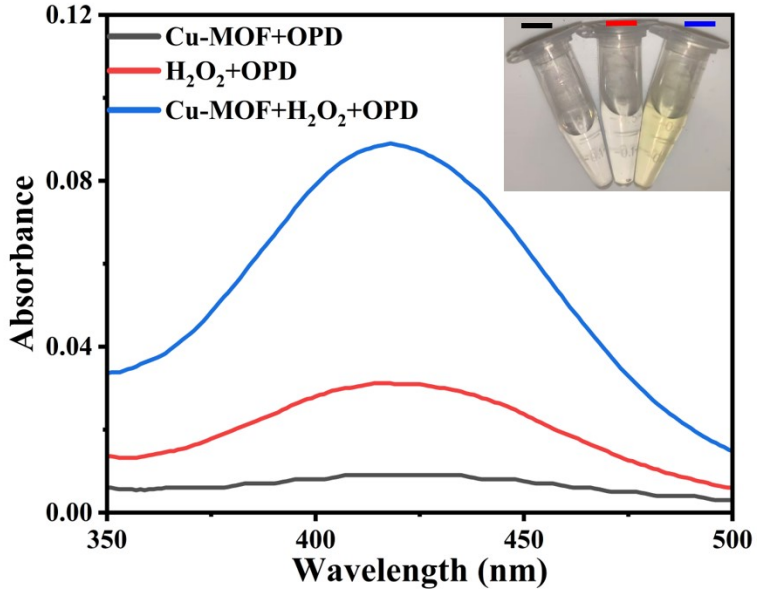


Fig.S3 UV absorption spectra of different systems (illustration: corresponding color photos taken under sunlight).

## 5. The Interaction between Cu MOF, OPD, and RB

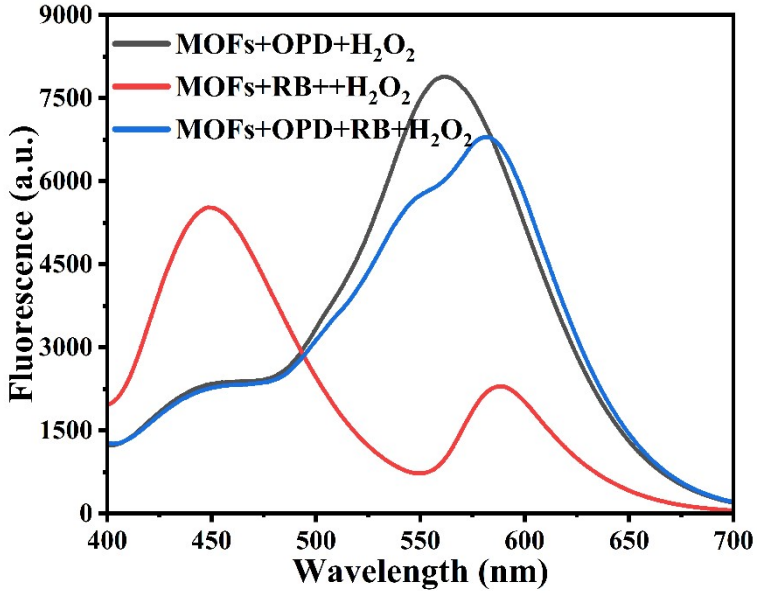


Fig.S4 Fluorescence spectra of different systems.

## 6. Optimization of detection conditions

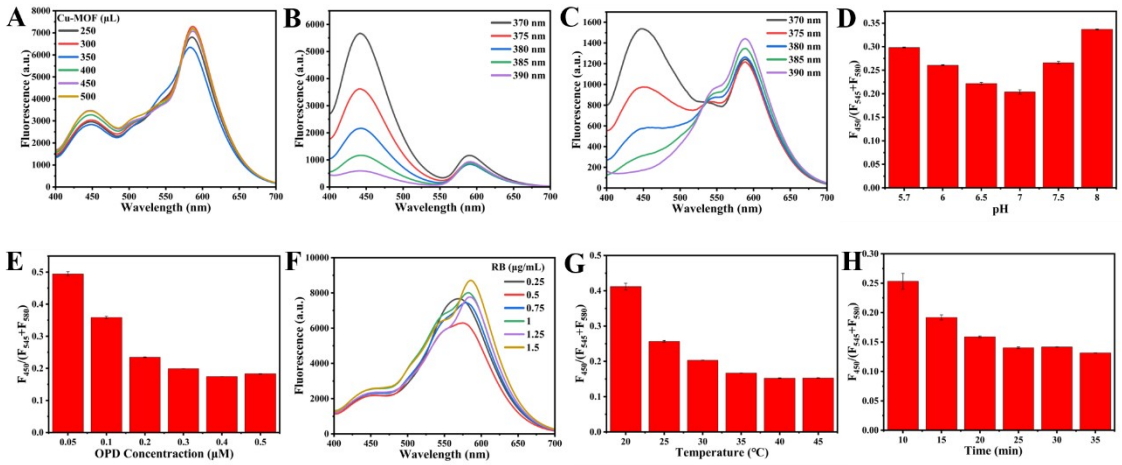


Fig.S5 The effect of Cu-MOF dosage (A); excitation wavelength (B and C); pH(D); OPD and RB concentration (E and F); temperature and time (G and F); on fluorescence detection system.

## 7. Linear relationship for GSH sensing

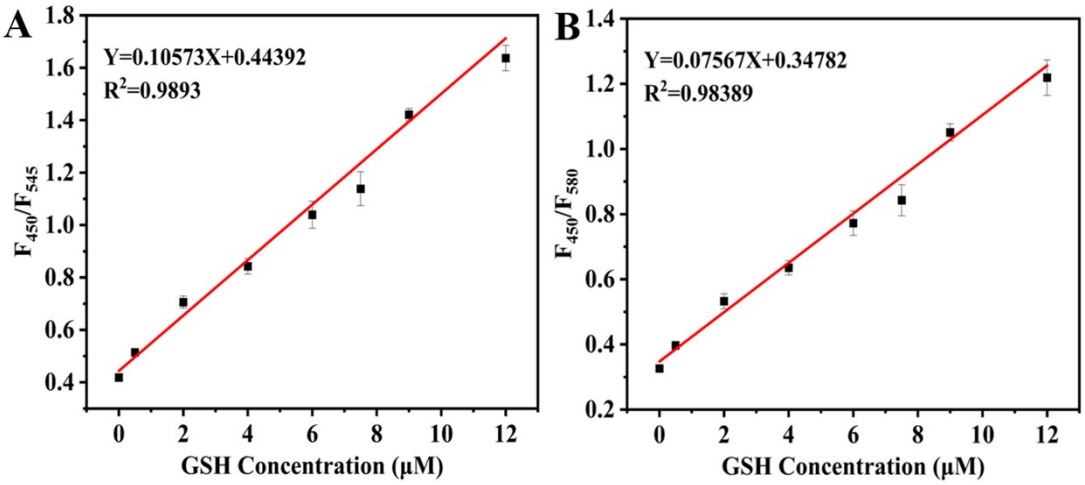


Fig.S6 The linear relationship between the $F_{450}/F_{545}$ value and the GSH concentration, and between the $F_{450}/F_{580}$ value (B) and GSH concentration.

## 8. Machine learning

8.1 Interpretability of Model Output

(1) Extract principal components with eigenvalues greater than 1, and ultimately extract 2 principal components with a cumulative variance contribution rate of 96.8% to achieve dimensionality reduction of 3D fluorescence signals; (2) Construct a 3D discriminant model using the reduced PCA principal components as input; (3) Regarding the interpretability of the model output, $F_{450}$ is the core channel that distinguishes GSH from other interferents (contributing 89.67% to the first principal component). This is because the inhibitory effect of GSH on the catalytic activity of Cu MOF specifically restores the $F_{450}$ signal, while AA, Cys, and UA significantly restore F450 compared to GSH; $F_{545}$ and $F_{580}$ are auxiliary discrimination channels, mainly used to distinguish fingerprint features between different interferences. The synergistic effect of the three achieves accurate recognition of GSH.

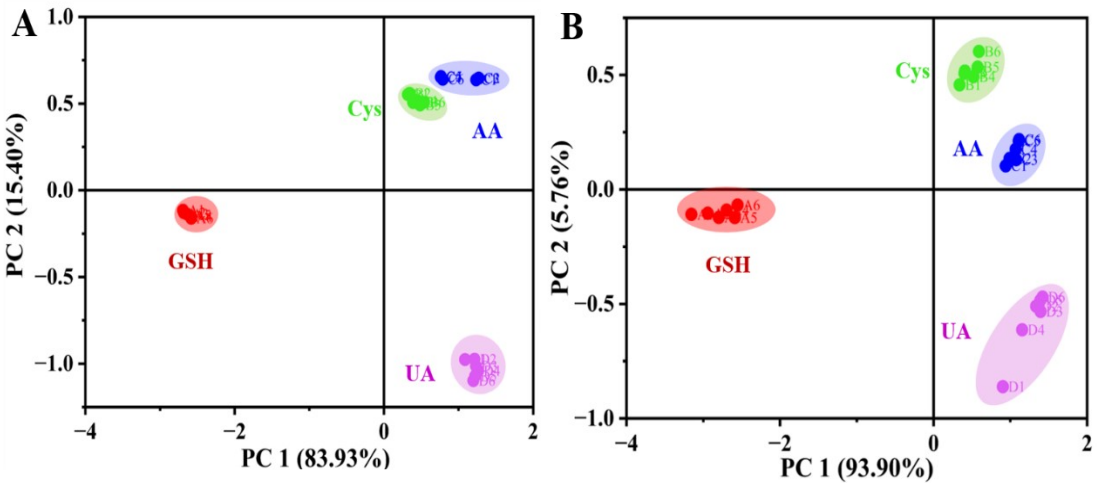


Fig.S7 PCA score plots of four different substances at concentrations of 5 μM (A) and 10μM (B)

## 9. Detection of GSH in real samples

9.1 Matrix effect analysis

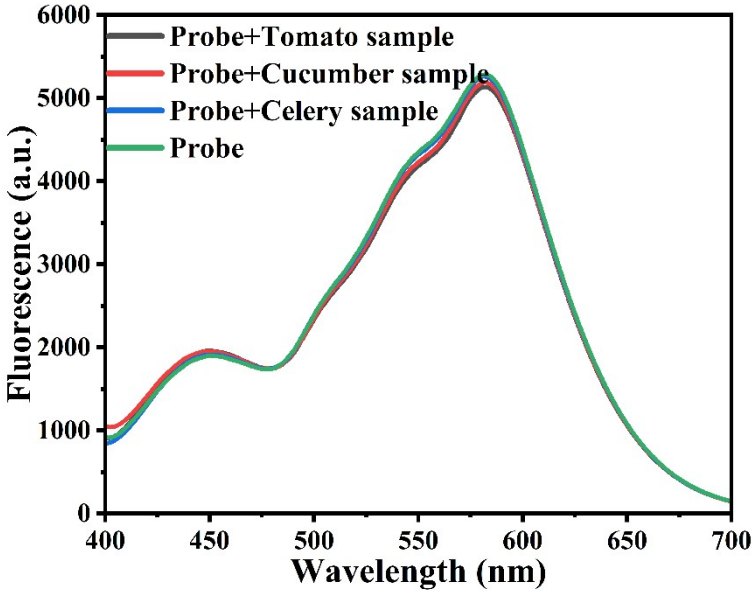


Fig.S8 The effect of 50 μL real samples on fluorescence detection system

9.2 Statistical calculation

According to the data in Table 1, the difference $d_i$= Found(Fl)- Found(HPLC) = [0.01, -0.03, 0.07, 0.04, -0.04, 0.12, 0, -0.05, -0.09]. The mean, standard deviation, and standard error of the difference values calculated sequentially are 0.0033, 0.065, and 0.0217, respectively. T=mean/standard error=0.153, degrees of freedom df=n-1=8. Check the distribution table of t, t0.05, 8=2.306. Due to the calculated t=0.153<2.306, P>0.05. P > 0.05, This indicates that there is no statistically significant difference in the measurement results of the two methods at the 95% confidence level.

## 10. Comparison of POD-like activity of Cu-MOF

**Table S1.** Comparison of the kinetic parameters of Cu-MOF, HRP and other nanozyme

| Catalysts | Substrate | Km (mM) | $V_{max}$ ($10^{-8}$ M $s^{-1}$) | Ref |
|---|---|---|---|---|
| HRP | OPD | 0.59 | 4.65 | [1] |
| | $H_2O_2$ | 0.34 | 9.48 | |
| Fe3O4/CNC@MOF | OPD | 0.883 | 0.542 | [2] |
| | $H_2O_2$ | 0.171 | 0.893 | |
| Fe–$N_{800}$CS | OPD | 1.75 | 3.52 | [3] |
| | $H_2O_2$ | 7.20 | 37.01 | |
| Cu-MOF | OPD | 0.54 | 7.87 | [4] |
| | $H_2O_2$ | 0.178 | 2.56 | |
| ATP/C3N4 NSs | OPD | 0.73 | 2.35 | [5] |
| | $H_2O_2$ | 0.03 | 10.60 | |
| Cu-MOF | OPD | 0.194 | 14.676 | This work |
| | $H_2O_2$ | 0.065 | 12.566 | |

## 11. Comparison of analytical performance of GSH detection methods

**Table S2.** Comparison of the GSH detection characteristics of triple-emission ratio fluorescent probe with other fluorescent sensors previously reported in the literature.

| Sensors | Linear range (μM) | LOD (μM) | Ref |
|---|---|---|---|
| P1 | 0-40 | 3.47 | [6] |
| NCL-based sensor | 0-10 | 2.98 | [7] |
| Mn3O4-OPD-Cu NCs | 2-120 | 0.83 | [8] |
| Nitrogen-doped carbon quantum dots-MnO2 nanotubes | 3-22.5 | 5.44 | [9] |
| CsPbBr3@BBA QDs | 0-250 | 2.84 | [10] |
| BR-CDs | 30-500 | 5.27 | [11] |
| Ir-NBD | 20-300 | 1.32 | [12] |
| Cu-CDs | 0-150 | 1.13 | [13] |
| UiO-66-NH2MOF | 1-70 | 0.57 | [14] |
| Cu-MOF | 0-12 | 0.27 | This work |

## References


[1] X Liu, Q Wang, H Zhao, L Zhang, Y Su and Y Lv, Analyst, 2012, 137, 4552-4558, https://doi.org/10.1039/C2AN35700C.

[2] C Hou, L Fu, Y Wang, W Chen, F Chen, S Zhang and J Wang, Cellulose, 2021, 28, 9253-9268, https://doi.org/10.1007/s10570-021-04117-w.

[3] Z Han, Q Fu, N Wang and X Su, Talanta, 2024, 272, 125704, https://doi.org/10.1016/j.talanta.2024.125704.

[4] H Yu, H Wu, X Tian, Y Zhou, C Ren and Z Wang, RSC Adv., 2021, 11, 26963-26973, https://doi.org/10.1039/D1RA04877E.

[5] M Liu, H Zhang, X Zhang, S Chen, Y Yu and J Wang, Anal. Chem., 2021, 93, 9002-9010, https://doi.org/10.1021/acs.analchem.1c02010.

[6] W Lang, Z Wu, J Li, Y Chen and Q Cao, Sens. Actuators, B, 2024, 412, 135772, https://doi.org/10.1016/j.snb.2024.135772.

[7] T Jin, M Cui, D Wu, W Zhu, Y Xu and X Qian, Chin. Chem. Lett., 2021, 32, 3899-3902, https://doi.org/10.1016/j.cclet.2021.06.033.

[8] H Lu, X Zhang, L Liu, L Zhu, X Xiong and T Xiao, Microchem. J., 2025, 209, 112801, https://doi.org/10.1016/j.microc.2025.112801.

[9] A Kujur, M Satnami, Y Chawre, P Miri, A Sinha, R Nagwanshi, I Karbhal, K Ghosh, S Pervez and M Deb, RSC Adv., 2024, 14, 20093-20104, https://doi.org/10.1039/D4RA03287J.

[10] J Sun, Q Li, X Li, X Yan and G Wang, Microchem. J., 2024, 199, 110043, https://doi.org/10.1016/j.microc.2024.110043.

[11] Y Wan, S Li, J Wang and F Pi, Food Chem., 2025, 475, 143337, https://doi.org/10.1016/j.foodchem.2025.143337.

[12] X Mu, M Li and F Fu, Biosens. Bioelectron., 2024, 246, 115901, https://doi.org/10.1016/j.bios.2023.115901.

[13] S Wu, Y Li, S Wang, H Lu, S Zheng, S Sun and S Xu, Spectrochim. Acta, Part A, 2025, 345, 126818, https://doi.org/10.1016/j.saa.2025.126818

[14] N Wang, M Xie, M Wang, Z Li and X Su, Talanta, 2020, 220, 121352,

https://doi.org/10.1016/j.talanta.2020.121352